Transactions of the Institute of Measurement and Control 26, 4 (2004) pp. 293–310

Investigation of an inertial-sensor-based dynamic position measurement system for a parallel kinematic machine

Jian Gao, Phil Webb and Nabil Gindy

School of Mechanical, Materials, Manufacturing Engineering and Management, The University of Nottingham, University Park, Nottingham NG7 2RD, UK

The key to the positional accuracy of a Parallel Kinematic Machine (PKM) is the precision to which the lengths of the individual parallel links (or struts) can be measured. The strut length can be measured to a high degree of precision using a laser interferometer but this is expensive. Alternatively, encoders may be used to measure the relative change in length of the strut but they can only record ball screw or motor rotation, and cannot detect any deformations that may occur within the machine's structure. In addition, only limited information on any dynamic disturbances such as vibration can be obtained. To obtain this type of data, displacement should be directly measured at the end of the strut. The use of inertial sensors offers a possible solution since they are self-contained, relatively low cost and can be easily mounted on the machine structure. However, an inherent limitation of inertial systems is the growth, with time, of errors in measured velocity and position; in the system described within this paper, they are corrected by using an external reference measurement and Kalman filtering. Through the integration of the two measurement systems, a velocity profile containing improved dynamic information can be calculated. The key steps required for the integration of the inertial and encoder measurement systems are introduced, and include the formulation of a system and measurement model and Kalman filter estimation and testing. In order to investigate the feasibility of the proposed measurement system, it was evaluated using a single PKM strut. The experimental results are presented and analysed.

Address for correspondence: Jian Gao, School of Mechanical, Materials, Manufacturing Engineering and Management, The University of Nottingham, University Park, Nottingham NG7 2RD, UK. E-mail: Jian. Gao@nottingham.ac.uk

 10.1191/0142331204tm122oa

Key words: dynamic measurement; inertial sensors; Kalman filter; Parallel Kinematic Machines (PKMs); position and orientation estimation.

1. Introduction

In recent years, there have been significant developments in the application of parallel kinematic structures to machine tools. A Parallel Kinematic Machine (PKM) consists of a number of links, connected together at the top and bottom by two platforms. If the lengths of the links are varied, then the position of the two platforms will change relative to each other. A PKM potentially possesses considerable inherent advantages compared to traditional (serial link) machine tool structures, as they are more rigid, more agile and can be much more accurate (Whittingham, 1998).

The individual struts usually comprise a ball screw and a DC servomotor. The key to a PKM's positional accuracy is the precision to which the lengths of these can be measured. The strut length can be measured by a laser interferometer to achieve a high degree of precision (Soons, 1997) but this method is expensive. Alternatively, encoders may be mounted on either the drive motor shaft or on the ball screw and used to measure the relative change in length. Encoder-based methods can only measure ball screw rotation and cannot measure any deformation of the structure caused by mechanical effects such as backlash, wear and thermal expansion. In addition, only limited information on the presence of any dynamic disturbances such as vibration can be obtained. Any resulting strut length measurement errors will be propagated to the calculated position of the Tool Centre Point (TCP) through the forward kinematic model with a resulting decrease in positional accuracy.

Inertial sensors such as accelerometers and gyroscopes are widely used in navigation systems to provide vehicle guidance information. They have also been applied to industrial robot applications (Janocha and Diewald, 1995) and machine tool calibration (Honeywell, 1994). Since the accuracy required for machine tools is far higher than that needed for navigation, high-grade inertial sensors are normally used. The cost of such systems has tended to limit their practical applications in industrial robots and machine tools. However, recent developments in solid-state accelerometers have resulted in the availability of low-cost sensors that can provide valuable information in many positioning applications if suitable data processing methods are used (Barshan and Durrant-Whyte, 1995).

This paper describes the development and testing of an inertial measurement system and an assessment of its potential for use as a means for measuring PKM strut displacement.

2. Development of an inertial-sensor-based dynamic position measurement system

Whilst the final intended application of the system is for PKM strut measurement applications, it was decided that for development and testing a simple mechanical

system was needed. For this purpose, a single-axis system was used that consisted of a ball screw and DC servo motor. The use of a single fixed axis also allowed accurate reference measurements to be easily performed. The inertial measurement system consisted of a DC capacitive accelerometer, a 16-bit DAQ card and a combined amplifier and power supply. The strut motion was controlled using NextMove WorkBench software running on a digital signal processor (DSP) motion controller (Gao, 2002). To provide direct feedback from the motor, an encoder was mounted on the drive shaft and connected to a Heidenhain lK121 counting card. This allowed data to be gathered without interfering with the operation of the DC motor servo loop. A diagram of the complete test bed is shown in Figure 1.

In addition to the apparatus shown in Figure 1, a Renishaw laser interferometer was used to provide an accurate external measurement of system performance. The laser has a resolution of 0.001μm and accuracy within ± 1.1 ppm (Figure 2).

2.1 Selection of accelerometer

For a typical PKM, accelerations are likely to vary between a maximum of $2\,g$ and zero during constant velocity. Also, according to the inertial sensor uncertainty analysis introduced in Gao (2002), the sensor selection should also consider the measured signal quality. Based upon these specifications, two accelerometers, a Kistler 8304B2 capacitive accelerometer and a Kistler 8704B500 piezoelectric accelerometer, were selected and tested. Figures 3 and 4 show the measured signals for identical 100-mm movements of the strut. The signal from the 8704B500 accelerometer has a lower signal−noise rate than that of the 8304B2 accelerometer. For an inertial system to function properly, its noise floor must be less than the necessary sensing resolution (Figliola and Beasley, 1991). From the experimental comparison, the Kistler 8304B2 was selected for further tests. Table 1 shows its full specification.

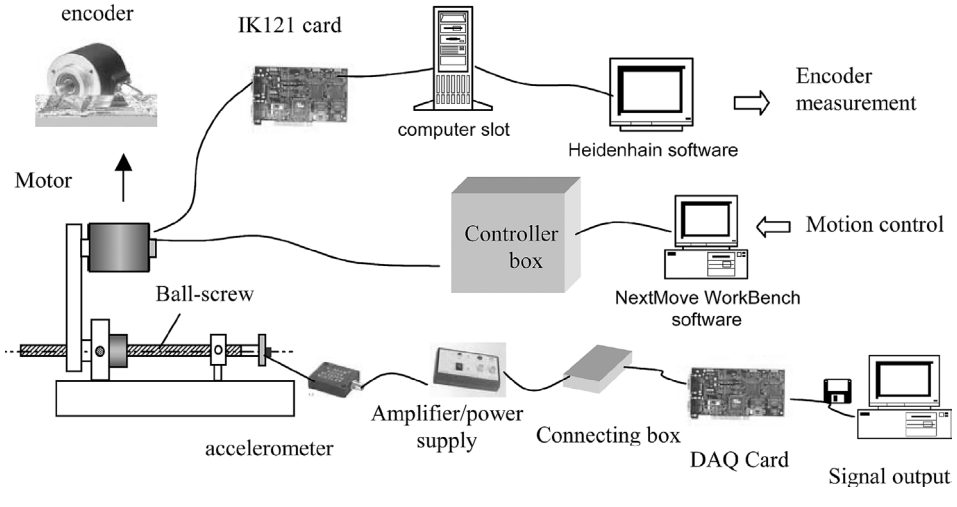

Figure 1 Diagram showing the experimental test bed

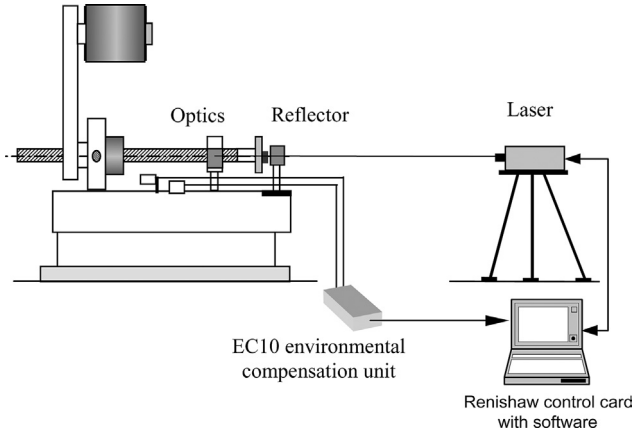

Figure 2 External measurement system

2.2 Accelerometer errors and misalignment

All inertial sensors are subject to a variety of errors that limit their accuracy. These errors are generally due to mechanical imperfections in the sensors and electrical imperfections in the associated instrumentation. Errors in the sensed measurement are processed in the same algorithms as the error-free component of the sensor output. These errors build up over time, corrupting the accuracy of the measurement data. Even the slightest offset errors of the sensors can cause extreme position errors. Therefore, data analysis and error reduction methods must be developed to minimize error effects and optimize system accuracy. To obtain accurate and reliable data, these errors must be quantified and compensated for. Each of the dominant sources of error and their mathematical representations are discussed below.

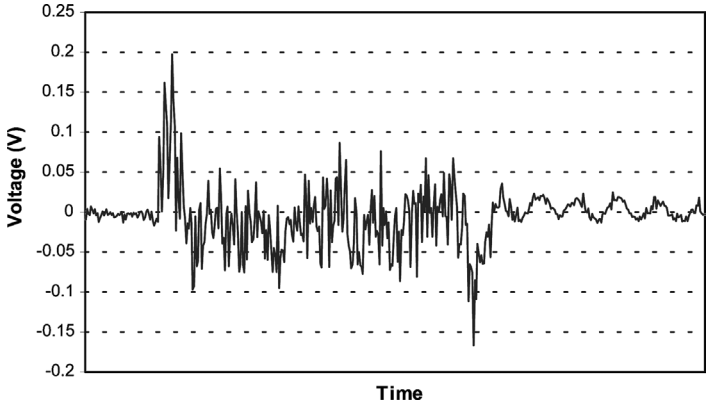

Figure 3 Kistler 8704B500 piezoelectric accelerometer output

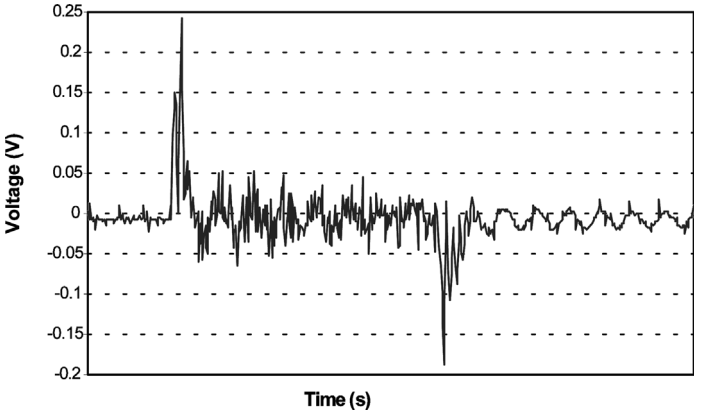

Figure 4 Kistler 8304B2 capacitive accelerometer output

2.2.1 Accelerometer measurement noise: Measurement noise from an accelerometer is mainly due to two principal causes:

- electrical noise—this can be modelled using white Gaussian noise of given standard deviation that depends on the circuit bandwidth;
- environmental noise—this noise is not white and the amplitude is usually higher than the electrical noise. This noise depends on vibration amplitude.

2.2.2 Accelerometer bias: Accelerometer bias is a bias or displacement from zero on the measurement of a specific force, which is present when the applied acceleration is zero. The size of the bias is independent of any motion to which the accelerometer may be subjected and is usually expressed in units of milli-g or micro-g depending on the precision of the device involved.

Since accelerometer bias will be treated in the same way as the real signal, it will result in unbounded velocity and position error growth through the data transformation and numerical integration process. The zero-g bias error will shift the sample mean value away from the true mean value of the measured variable by a fixed amount. The bias accumulates into displacement errors according to the following equation

$$\Delta d = \frac{1}{2} b_a t^2 \tag{1}$$

Table 1 Kistler 8304B2 accelerometer specification

Acceleration range	$\pm 2g$
Zero-g output	2.5 V
Resolution	140μg
Frequency response	0 ... 300 Hz
Transverse sensitivity	$<1\%$
Sensitivity	1000 mV/g

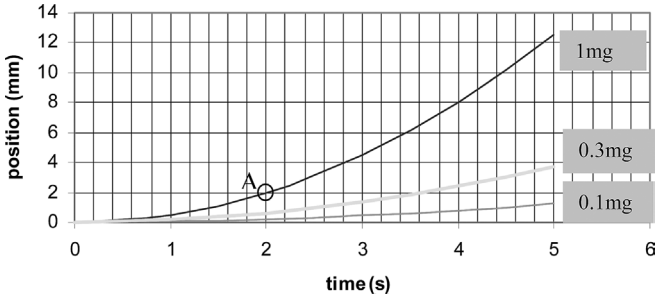

Figure 5 Accelerometer-induced position error

where b_a is the bias acceleration, Δd is the displacement error induced by the bias through the travelling time t.

The kinematic equation (1) shows that an uncompensated accelerometer bias builds up displacement error as a function of the time squared (supposing that the initial velocity is zero). Figure 5 shows the position errors caused by different accelerometer biases. Point A shows the position error of 2 mm caused by a 1-mg accelerometer bias error over 2 s.

The accelerometer bias is highly temperature sensitive and may vary from day to day by as much as 10 times more than in-run random drifts (Grafarend, 1989). It may also slowly change over time, perhaps from the ageing of internal components. As variations occur in the ambient temperature, the zero-g bias will exhibit some temperature drift. When an accelerometer is used to measure low g levels over wide temperature ranges, the zero-g drift can become large in proportion to the signal amplitude. For the accelerometer (8304B2) used in this paper, the temperature performance of the bias drift is shown in Figure 6, and it is measured in units of the form:

$$K_{oT} = 0.002g/^{\circ}\mathrm{C} \text{ (reference temperature is } 22^{\circ}\mathrm{C})$$

2.2.3 Accelerometer scale factor error: Accelerometer scale factor error may be expressed as a percentage of the measured full-scale quantity or simply as a ratio. Scale factor drift defines the amount by which an accelerometer's sensitivity varies as the ambient environmental conditions change. These conditions could be the temperature or frequency related to the measurement. Thermal effects on scale factor error can be very significant and are often difficult to model accurately. Therefore in very accurate inertial systems, it is often necessary to control the temperature of the sensors very precisely (Titterton and Weston, 1997). Solid-state sensors are not as seriously affected as mechanical sensors, but temperature effects do still cause scale factor errors.

As variations occur in the ambient temperature as well as that of the internal components, the scale factor error will change (Figliola and Beasley, 1991). The sensitivity of the accelerometer used in this work is 1000 mV/g under standard ambient conditions of temperature and frequency. From the calibration

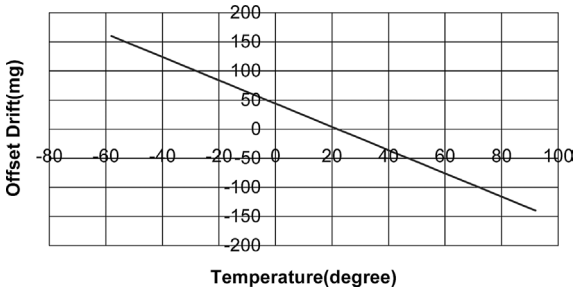

Figure 6 Effect of temperature on accelerometer zero-g bias

information specified by the sensor supplier, the calculated scale factor drift with temperature is shown in Figure 7. The temperature coefficient of the sensitivity is specified as

$$K_{S_T} = 0.02\%FS/^{\circ}\mathrm{C}(\text{reference temperature is } 22^{\circ}\mathrm{C}) \tag{2}$$

The corresponding sensitivity drift e_{SF} under the measure temperature (T°C) can be calculated from the expression

$$e_{SF} = K_{S_T} \cdot \Delta T \quad (g) \tag{3}$$

where K_{S_T} represents temperature coefficient of the scale factor, $\Delta T = T^{\circ}\mathrm{C} - 22^{\circ}\mathrm{C}$ is temperature deviation, T°C is the ambient temperature of measurement.

Besides the errors described above, accelerometer nonlinearity, cross-axis coupling error and threshold can also affect the real measurement quality and decrease the achievable system accuracy.

2.2.4 Misalignment error: Inertial sensors attached to the strut, or any machine, will resolve their measurements relative to the inertial space along the sensitive axes of the instruments. Perfect alignment with their assumed directions is not possible under realistic conditions. Identification of the misalignment matrices to transform between the instrument and platform frames is a primary objective of the IMU (inertial measurement unit) alignment process (Chatfield, 1997). If the

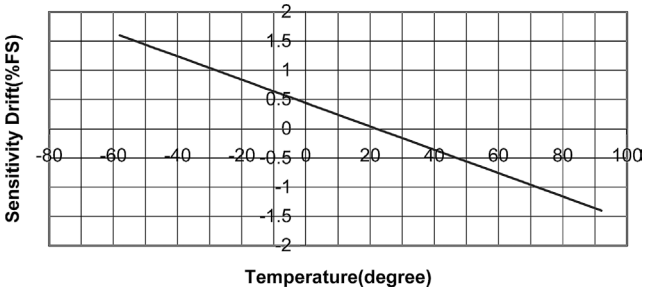

Figure 7 Temperature performance of accelerometer sensitivity

accelerometer were to be mounted on a PKM strut to measure its horizontal motion then in theory, the accelerometer should only measure the acceleration along its sensing axis. However, the strut may not be horizontal and may tilt at a small angle along its axis; hence the accelerometer will sense an acceleration component due to gravity. Since the angle will not disappear during the movement of the strut, the gravity component contaminating the output of the accelerometer will be treated as a part of the acceleration, and thus build up position errors as time t^2 (Equation 6). Assuming the misalignment angle along the sensitive axis is β shown in Figure 8, the component of gravity in the accelerometer data at the initial position will be

$$a_x = g \sin \beta \tag{4}$$

Thus, a velocity and position error caused by the misalignment is

$$V_x = a_x t = g \cdot \sin \beta \cdot t \tag{5}$$

$$P_x = \frac{1}{2} a_x t^2 = \frac{1}{2} \cdot g \cdot \sin \beta \cdot t^2 \tag{6}$$

For example if the tilt angle is $\beta = 0.05^\circ$, and the time of the motion varies between 0.5 and 3 s, then the position error will be between 1 and 36 mm. Therefore, the misalignment error is significant, especially for a long distance movement. To obtain the initial alignment acceleration, a tilt sensor is required to provide the initial angle of the accelerometer relative to its sensing axis. The expected acceleration due to gravity can then be determined and compensated for during alignment.

2.3 Signal processing and error correction

To compensate for all the quantified errors, a signal processing and error correction algorithm was devised and implemented (Gao, 2002).

2.3.1 Accelerometer error correction: It is known from the previous error analysis that the accelerometer measurements contain errors from manufacturing,

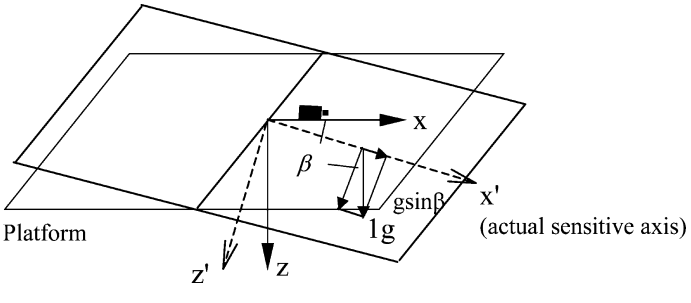

Figure 8 Gravity component contained in acceleration data due to initial misalignment

system set-up, environmental factors and other random sources. Errors in the sensed measurements are processed in the same algorithms as the error-free component of the sensor output and hence corrupt the accuracy of the measurement and the derived position data.

To improve the quality of inertial measurement system, a number of error correction methods were developed, the application of these is shown diagrammatically in Figure 9. Among these methods, a low-pass finite impulse response (FIR) filter was designed to filter the high-frequency noise of the accelerometer data. The systematic errors including the accelerometer bias, scale factor error and misalignment are predictable, and therefore can be compensated for. A bias error model was built to remove the accelerometer bias (Gao, 2002).

Whilst the application of the compensation model reduced the error levels within the system a number still remain that coincide with the signal of interest and will therefore be amplified through the numerical integration process and cause waveform distortion. To help correct the remaining errors, a velocity reconstruction method was developed based upon the physical machine motion (Gao *et al.*, 2003). However, errors in the inertial system cannot be fully eliminated and will tend to grow with time. One method of reducing this residual error is by

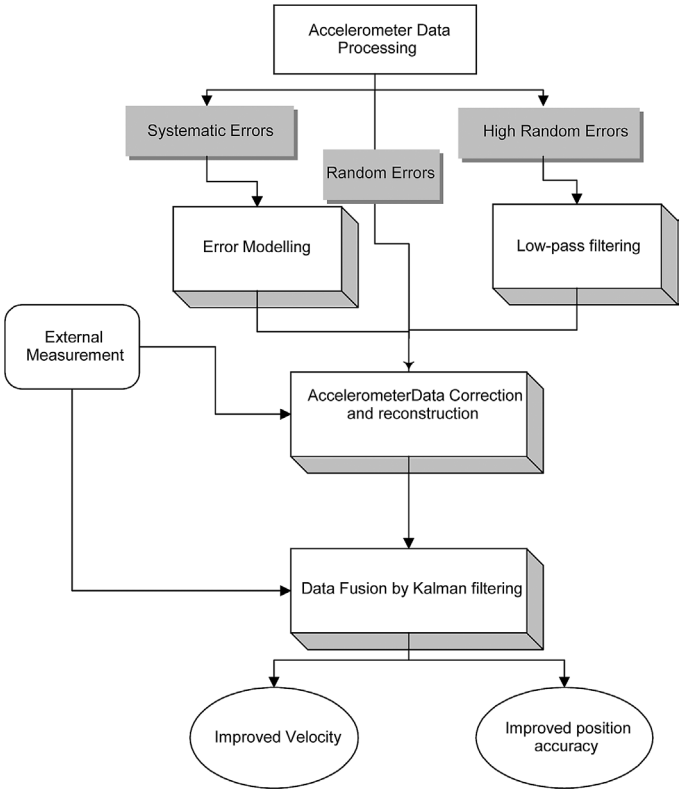

Figure 9 The procedure of accelerometer data processing

periodically updating the inertial system with an external measurement signal. In this application, the encoder measurements can be used to periodically update the inertial system. In the system described here, data from the ball screw encoder measurement was used as the external input. One of the reasons for the choice of encoders as an external source is their availability, since encoders are used in machine tools to provide position or velocity information. They are also used in most PKMs to provide strut length. The inertial system can also provide dynamic error compensation for the encoder measurement. Since the inertial system directly measures the dynamic motion, and the encoder measurement system only provides calculated position data without any dynamic information about the motion, it is therefore possible to obtain an improved velocity profile through the integration of the inertial and the encoder measurement systems. In this application, the Kalman filtering statistical technique was adopted to fuse the two sources of data and should theoretically provide 'the best of both worlds' (Brown and Hwang, 1998).

3. Application of a Kalman filter for measurement data fusion

The implementation of the inertial/encoder integration system and Kalman filter is summarized in Figure 10. The following sections describe the establishment of the system model, the measurement model of the linear inertial system and the initial parameter settings for the Kalman filter.

3.1 The system model

In the inertial measurement system, the measured acceleration, velocity and position were selected as the system state variables. Thus, the state vector can be described as

$$X = [\, x \quad x_v \quad x_a \,]^T \tag{7}$$

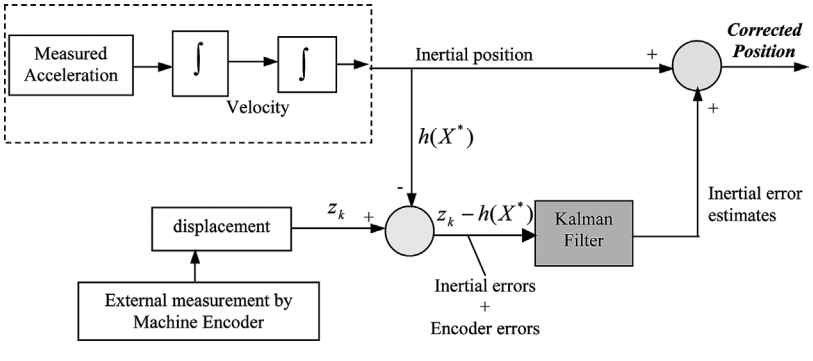

Figure 10 Implementation scheme of the inertial/encoder integration system for the linear measurement along one-axis direction

and the inertial positioning system equation can be stated as:

$$\mathrm{x}(k+1) = \begin{bmatrix} 1 & T & \frac{1}{2}T^2 \\ 0 & 1 & T \\ 0 & 0 & 1 \end{bmatrix} \begin{bmatrix} x \\ x_v \\ x_a \end{bmatrix} + \begin{bmatrix} 0 \\ 0 \\ w(k) \end{bmatrix} \tag{8}$$

where x is the linear position error; x_v the velocity error and x_a the acceleration error, $x_a = \Delta a$. When the movement is not in a horizontal direction, the accelerometer is influenced by gravity. T is the sampling interval and $w(k)$ is the input white noise with zero mean and unknown covariance matrix.

3.2 The measurement model

The measurement model describes the relationship of the encoder measurement with the state vectors of the inertial system. For the encoder position measurement system, the measurement model can be expressed as:

$$\begin{aligned} \mathrm{z}(k) &= \mathbf{h}(\mathbf{x}(k)) + \mathbf{v}(k) \\ &= \mathrm{H}(k)\mathbf{x}(k) + \mathbf{v}(k) = \begin{bmatrix} 1 & 0 & 0 \\ 0 & 0 & 0 \\ 0 & 0 & 0 \end{bmatrix} \begin{bmatrix} x \\ x_v \\ x_a \end{bmatrix} + \begin{bmatrix} v(k) \\ 0 \\ 0 \end{bmatrix} \end{aligned} \tag{9}$$

where $\mathbf{z}(k)$ is the measurement vector, encoder position measurement, $\mathbf{v}(k)$ the additive measurement white noise with zero mean and known covariance matrix, and $\mathbf{H}(k)$ the transition matrix, giving the ideal (noiseless) connection between the measurement vector $\mathbf{z}(k)$ and the state vector $\mathbf{x}(k)$.

3.3 Initial value and covariance

Kalman filtering is a recursive procedure and therefore knowledge of the initial conditions is required prior to the estimation (Kalman, 1960; Brown and Hwang, 1998). At an initial epoch t_0, the Kalman filter is initialized with the initial estimates of the error covariance matrix P_0 and the initial state vector $\mathbf{x}_0$. At the starting point, the state vector is usually unknown. However, knowledge of the initial state vector may have been derived from measurements or as a result of a previous (filter) adjustment.

The initial value of P_k^- is shown to affect the results achieved in the update stage, dictating how quickly the algorithm will converge on parameters within an acceptable error. Brown and Hwang (1998) suggested that if there is no initial predicted estimate, P_k^- should be initialized to the covariance of the first measurement, although this method is misleading in that it shows increasing error the further the first located point is from the external origin. However, experiments performed in this research have shown that initializing P_k^- with the covariance of the error

obtained from this method provides a starting estimate that is too low, causing the K_k matrix to decrease immediately, effectively eliminating error gain from subsequent measurements. Therefore it is important to initialize P_k^- to values high enough to allow influence from measurements taken from the encoders early in the sequence so that the filter can self-adjust according to the input data. It is noted in Bozic, (1994) that initializing the error covariance is not an exact science. P_0 is the initial covariance matrix, which can be determined by the matrix:

$$P_0 = \begin{bmatrix} \delta_{x_0}^2 & 0 & 0 \\ 0 & \delta_{v_0}^2 & 0 \\ 0 & 0 & \delta_{a_0}^2 \end{bmatrix} \tag{10}$$

where $\delta_{x_0}^2$ represents the initial position uncertainty, $\delta_{v_0}^2$ represents the initial velocity uncertainty and $\delta_{a_0}^2$ is the initial accelerations uncertainty.

The other quantities that must be known before estimation can begin are: the system model matrices, Φ_k and Q_k, and the measurement model matrices, H_k and R_k

H_k is initialized to enable conversion of the state parameters to the same basis as the measurement data. Here, the **H** matrix is just an identity matrix, only position data is extracted, so $\mathbf{H} = [\mathbf{I}, 0]$. R_k is the variance of the external measurements and depends upon the accuracy of the measurements. If the measurement has an accuracy of 0.01 m, then the value can be set $R_k = (0.01)^2 \text{m}^2$. Q_k is the process noise variance, which can be expressed as (Farrell and Barth, 1998):

$$Q_k = \sigma \begin{bmatrix} \frac{t^4}{20} & \frac{t^3}{8} & \frac{t^2}{8} \\ \frac{t^3}{8} & \frac{t^2}{3} & \frac{t}{2} \\ \frac{t^2}{6} & \frac{t}{2} & 1 \end{bmatrix} \tag{11}$$

where σ represents the standard error of the measured accelerometer data, and t is the time step of the Kalman filter.

Based upon the system model, the measurement model, their matrices, the initial values of the state vector x_0 and the covariance error P_0, the Kalman filter recursive algorithm was then be implemented and tested.

3.4 Estimate errors

The achievable result including position and velocity profile estimates are dependent on the Kalman filter tuning. Through filter tuning it can be observed whether the filter's actual performance is consistent with the behaviour of its associated covariance matrix P. This is demonstrated by the fact that the estimated states shown in Figures 11–13 tend to remain between the two standard deviation bounds for each of the states. The standard deviation bounds are defined by the square roots of the corresponding diagonal elements in the computed P matrix (standard deviation $\sigma = \pm\sqrt{P_{ii}}$). If the estimation error exceeded the two-sigma

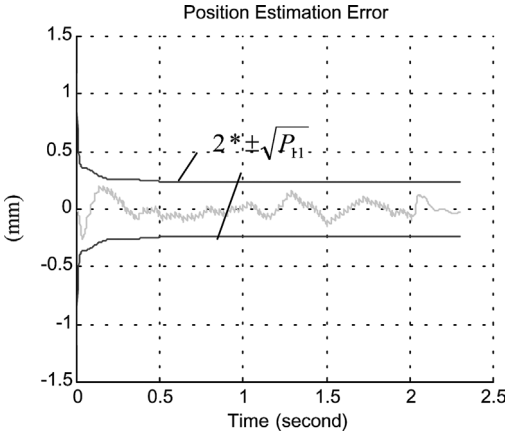

Figure 11 Position estimation

bound, then the performance of the Kalman filter under the parameter setting was unacceptable.

In this application, since the inertial dynamic measurements are very noisy, the process noise variance Q needs to be set to a high value to obtain a large filter gain to achieve an accurate position estimate close to the encoder measurement. However, to provide extra dynamic information for the velocity profile, the filter gain should weight some of the inertial dynamic measurement, so as to make the velocity estimate contain real dynamic information. Therefore, a trade-off between the expected position accuracy and dynamic velocity profile needs to be considered in the tuning process.

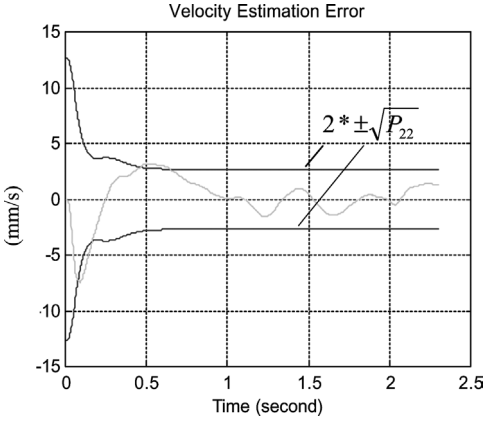

Figure 12 Velocity estimation

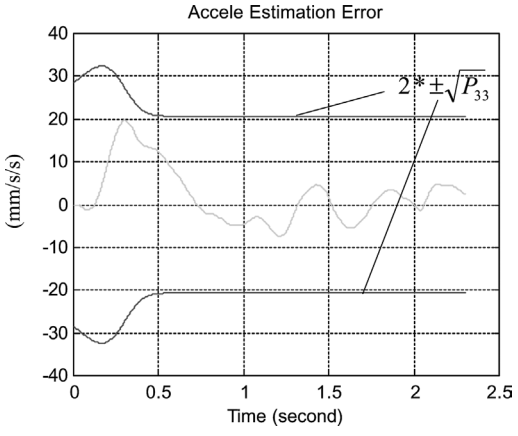

Figure 13 Acceleration estimation

3.5 Filter consistency

Because of the importance of setting the value of Q and R to satisfy the dynamic model, tuning processes are necessary to adjust the parameters for the Kalman filter to achieve good performance and consistency. Based upon the integration system model and initial value settings, the filter can be implemented to estimate the states of interest. However, unless the true values of those states are known, there is no way of determining whether the filter is computing correct estimates. The only information available from the behaviour of the filter is the difference between the observation and the predicted observation, that is, the innovation v_k represented in Equation (12).

$$v_k = \mathrm{z}_k - \mathrm{H}_k \hat{\mathrm{x}}_k^- \tag{12}$$

The innovation v_k has the property that it must be both unbiased and white, and have covariance S_k if the filter is operating correctly. To determine whether this is the case, the innovation is normalized,

$$\varepsilon_k = v_k^T \mathrm{S}_k^{-1} v_k \tag{13}$$

ε_k is called the normalized state estimation error squared. If the filter assumptions are correct then the samples of ε_k are distributed as an χ^2 distribution in n_x degrees of freedom, where n_x is the dimension of state vector $\boldsymbol{x}$, then (Julier, 1997; Yaakov and Tomas, 1998):

$$E[\varepsilon(k)] = n_x \tag{14}$$

Instead of using Equation (13) as a method of determining filter consistency, it can be used as a gating function. When an observation is obtained, Equation (13) is formed, and if the value ε_k is less than a predefined threshold, then the observation is accepted. This allows for a means of detecting any faults within the observation.

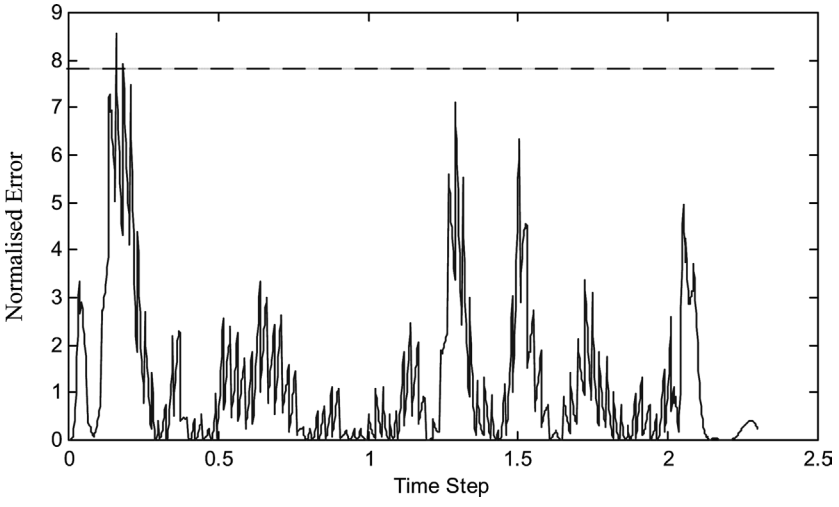

Figure 14 Normalized state error squared ($Q = 1.0^2$) with 95% confidence region. Only three are out of the 95% confidence range ($r = 7.81$)

The threshold value is obtained from standard χ^2 tables and is chosen based on the confidence level required. For a single run, the 95% confidence region can be used to check the behaviour of the normalized state error squared with process noise variance. For example, at a 95% confidence level, for a state vector that includes three state variables of the system, then the confidence region is $\varepsilon_k = 7.8$ (Yaakov and Tomas, 1998). Therefore, for a three-degree-of-freedom chi-square random variable, it has $P\{\chi_3^2 \leq 7.8\} = 0.95$. If the filter is matched to the system, the estimate error should fall in the confidence region at least 95% of the time.

A formal test for consistency is to examine the normalized state error. A number of single-run tests were performed with different process noise variance Q to check the Kalman filter consistency. For a process noise variance value of $Q = 1.0^2$ $(\mathrm{m/s^2})^2$, the normalized state error squared is shown in Figure 14. As described above, the confidence region for a three-degree-of-freedom state vector is 7.81 at a 95% confidence level. The filter had only three points out of 1149 to be outside the 95% confidence region, clearly an acceptable situation. However, when the process noise variance had a value of $Q = 0.01^2(\mathrm{m/s^2})^2$, the filter had practically 90% points were outside the confidence region, which illustrates the serious mismatch.

4. Result comparison

For the accelerometer used in this system, the maximum usable sampling frequency is 600 Hz based on the sensor's frequency response, but to improve the waveform integration accuracy of the measured data, a sampling frequency of 1000 Hz was used. The Renishaw laser position system was used as a standard ref-

Table 2 STD position errors (unit: mm)

Test bed	Raw data	Filtered data	Velocity corrected data
300 mm	41	38	16

erence for the inertial measurement. The initial experiments were performed using 300-mm movement.

Table 2 shows the inertial position results from the original accelerometer data and from the data corrected by the low-pass FIR filter and the velocity reconstruction method.

Based upon the initial parameter settings and Q, R tuning in the Kalman filter, the result of the estimated position errors over 20 runs is shown in Figure 15 for a 300 mm movement. Compared with the position result from the raw accelerometer data, the standard deviation position error through the Kalman filtering was greatly reduced from 41 to 0.15 mm for the 300-mm movement. If the inertial data were pre-corrected by the low-pass filter error model and the velocity reconstructing method, the positional accuracy was improved to 0.12 mm (compared in Figure 16).

The use of the Kalman filter significantly improves the performance of the inertial system but this is at the expense of the accuracy of the combined measurement when compared with the encoder system. However, the Kalman filter estimation can also provide information on the actual behaviour of the end of the strut. The estimated velocity information contains the machine dynamic information, such as the machine vibration and backlash. The velocity profile from the Kalman filter integration system is shown in Figure 17, and is compared with the reference velocity profile from the laser interferometer and with the encoder velocity profile. From the velocity comparison, it can be seen that the encoder measurement does not contain any dynamic information and that the estimated velocity profile is closer to the laser reference profile.

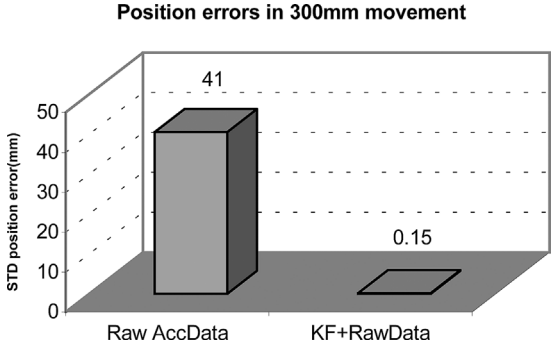

Figure 15 The estimated position errors by Kalman filter compared with the result from raw accelerometer data for 300-mm movement in PKM strut tests

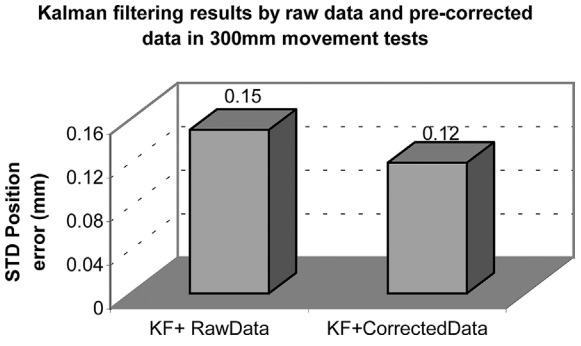

Figure 16 The inertial/encoder system results comparison by using the precorrected inertial data and raw data in the Kalman filtering for 300-mm measurement on PKM strut test bed

5. Conclusions

The low-cost solid-state accelerometer used in this work was limited in its accuracy and performance and could not, on its own, provide a measurement system with sufficient accuracy for the proposed application. However, the inclusion of an accelerometer did prove useful in that it could provide extra dynamic information regarding the actual movement of the strut that was not registered by the remote encoder.

From the results obtained for the linear strut measurement, the inertial dynamic system could provide an accuracy of 120 μm if the inertial data is precorrected and

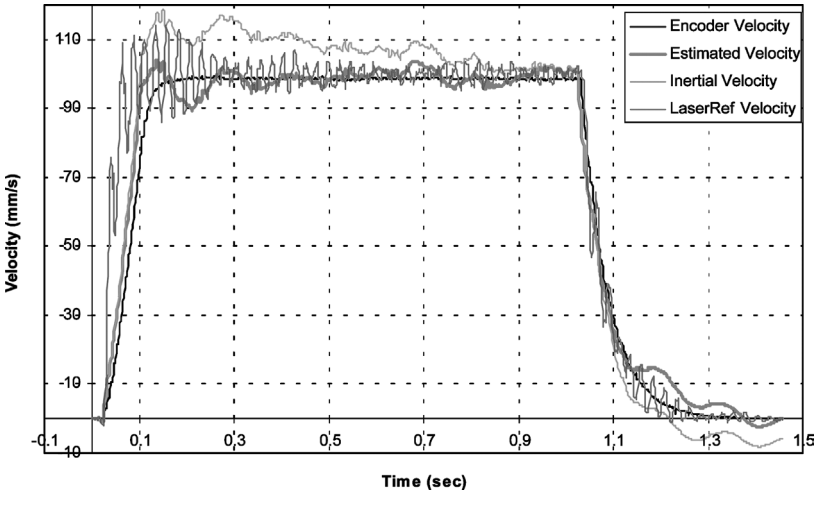

Figure 17 Dynamic information measured by inertial system, encoder device, laser interferometer and the Kalman filter estimation

Kalman filtered. Compared with the accuracy of 34.55 μm of the PKM strut with encoder measurement system only, the inertial system accuracy is not good enough in its current form to provide a complete replacement for the existing system. However, the developed inertial measurement system can obtain real dynamic information for the control system and can therefore be used to improve overall system performance. The experimental work presented shows that significant dynamic information, in this case vibration, is not captured by the encoder feedback system.

For more general PKM position measurement applications, the availability of an estimate of the actual machine position can considerably simplify the solution of the Kinematic equations; this can be obtained by mounting the inertial sensors on the moving platform. With further improvements in inertial sensor technology, or the employment of a high-grade sensor, the proposed inertial system could eventually produce the required accuracy and performance for PKM strut measurement applications.

References

Barshan, B. and **Durrant-Whyte, H.F.** 1995: Inertial navigation systems for mobile robots. *IEEE Transactions on Robotics and Automation* 11, 328–42.

Bozic, S.M. 1994: *Digital and Kalman filtering: an introduction to discrete-time filtering and optimum linear estimation*. London: Arnold

Brown, R.G. and **Hwang, P.Y.C.** 1998: *Introduction to random signals and applied Kalman filtering with Matlab exercises and solutions*. New York: John Wiley & Sons.

Chatfield, A.B. 1997: *Fundamentals of high accuracy inertial navigation*, Vol. 174. Reston, VA: American Institute of Aeronautics and Astronautics, Inc.

Farrell, J. and **Barth, M.** 1998: *The global positioning system and inertial navigation*. New York: McGraw-Hill.

Figliola, R.S. and **Beasley, D.E.** 1991: *Theory and design for mechanical measurement*. New York: Wiley.

Gao, J. 2002: Dynamic position sensing for parallel kinematic machine. PhD thesis, The University of Nottingham.

Gao, J. Webb, P. and **Gindy, N.** 2003: Error reduction for an inertial-sensor-based dynamic Parallel Kinematic Machine positioning system. *Measurement Science and Technology* 14, 543–50.

Grafarend, E. 1989: Geodetic positioning by inertial and satellite system: an overview. *High precision navigation*. Berlin: Springer.

Honeywell Technology Centre. 1994: Application of ring laser gyros to precision machine tools. Minneapolis, Minnesota.

Janocha, H., and **Diewald, B**. 1995: ICAROS: Over-all-calibration of industrial robots. *Industrial Robot* 22, 15–20.

Julier, S.J. 1997: Process models for the navigation of high-speed land vehicles. PhD thesis, University of Oxford.

Kalman, R.E. 1960: A new approach to linear filtering and prediction problems. *Transactions of the ASME, Journal of Basic Engineering* 82, 34–45.

Soons, J.A. 1997: Error analysis of a hexapod machine tool. *3rd International Conference and Exhibition on Laser Metrology and Machine Performance, Lamdamap*. Southampton: Computational Mechanics Publications, 347–58.

Titterton, D.H. and **Weston, J.L.** 1997: In Sheaman, E.D.R. and Bradsell, P. *Strapdown inertial navigation technology*. London: Peter Peregrinus Ltd.

Whittingham, B. 1998: Capabilities of parallel link machine tools: preliminary investigations of the Variax Hexacenterä. *ASME International Mechanical Engineering Congress and Exposition*. Anaheim, California.

Yaakov, B.S. and **Tomas, E.F.** 1998: *Tracking and data association*. New York: Academic Press.